Research article

Comprehensive mapping of Neurofibromin (NF1) expression in developing mouse brain

Vishal Lolam[1] and Achira Roy[1,*]

[1]Neurodevelopment Laboratory, Neuroscience Unit, Jawaharlal Nehru Centre for Advanced Scientific Research (JNCASR), India

***Correspondence:** Achira Roy, MSc, PhD
Assistant Professor
Neurodevelopment Lab, Room: SBS-B201, Neuroscience Unit,
Jawaharlal Nehru Centre for Advanced Scientific Research (JNCASR),
Rachenahalli Lake Road, Jakkur PO, Bangalore, India. PIN: 560064
achira.roy@jncasr.ac.in

Short Title: NF1 expression in mouse brain

Keywords: NF1, neurodevelopment, brain expression, cerebellum, single-cell reanalysis

Total number of words: 4820

Number of Figures: 9
Number of Supplementary Figures: 3

Abstract:

Neurofibromin (NF1) is a critical negative regulator of the RAS-RAF-ERK pathway, mutations in which have been clinically implicated in various neurodevelopmental disorders. However, the lack of a high-resolution spatiotemporal map has obscured the understanding of why specific cell populations and developmental processes are uniquely vulnerable to *NF1* loss. In this study, we present a comprehensive atlas of NF1 expression in the developing mouse brain. Using *in situ* hybridization and immunohistochemistry, we characterized NF1 distribution from early embryonic stages through postnatal maturation. We further integrated these findings with single-nuclei RNA-sequencing (snRNA-seq) datasets from adult mouse brain to achieve higher resolution. Our results reveal a previously undocumented graded expression pattern of NF1 across various brain regions and cell lineages. This comprehensive study will not only help understand the fundamental role of NF1 in brain development but will also be pivotal in providing a framework for studying *NF1*-associated brain disorders.

Summary statement:

Graded expression of Neurofibromin (NF1) identified across embryonic and postnatal stages reveals unique sub-lineages of neural cells in different parts of the developing mouse brain.

Introduction:

Neurofibromatosis type 1 is one of the most common autosomal dominant neurogenetic disorders, affecting approximately 1 in 3,000 individuals worldwide (Nix et al. 2020). The condition is caused by mutations in the *NF1* gene, which encodes neurofibromin, a large multifunctional protein that serves as a critical negative regulator of the RAS-RAF-ERK pathway (Karaconji et al. 2019). NF1 consists of RAS-GTPase activating (GAP) domain, which facilitates the conversion of RAS-GTP (Active) to RAS-GDP (inactive), thereby negatively regulating RAS function (Martin et al. 1990). Since the RAS-RAF-ERK pathway is important for cell growth, proliferation and survival, NF1 acts as a brake on cellular growth and proliferation (Cichowski & Jacks 2001). In patients suffering from Neurofibromatosis type 1, this brake is lost, resulting in the formation of benign or malignant tumours in the brain and brainstem (Albers & Gutmann 2009; Lucas et al. 2022; Ayasa et al. 2024). Interestingly, a significant proportion of these pediatric patients develop neurodevelopmental disorders such as cortical malformations, epilepsy, hydrocephalus, autism spectrum disorder, intellectual disabilities, and movement disorders (Balestri et al. 2003; Sorrentino et al. 2021; Roth et al. 2019; Plasschaert et al. 2015; Hyman et al. 2005; Rietman et al. 2017; Lolam & Roy 2025; Báez-Flores et al. 2023). These clinical findings underscore the importance of NF1 in neurodevelopment beyond its canonical role in tumorigenesis.

Despite the profound impact of *NF1* mutations on the functioning of the central nervous system (CNS), our understanding of the spatiotemporal dynamics of *NF1* expression during brain development remains incomplete. Previous studies have established that NF1 is essential for embryonic development, with null mice dying in utero between embryonic days (E) 12.5 and 13.5 due to cardiovascular defects (Brannan et al. 1994; Jacks et al. 1994). In addition, studies done by knocking out *Nf1* in cultured cells and in various model systems have demonstrated altered neurodevelopmental processes (Lakkis et al. 1999; Zhu et al. 2001; Gutmann et al. 1999; Sanchez-Ortiz et al. 2014; Shin et al. 2012; Durkin et al. 2023). However, the lack of a high-resolution spatiotemporal map has limited our ability to pinpoint which developmental processes or cell populations are most vulnerable to *Nf1* loss.

Although there are some reports of NF1 expression in the brain (Daston et al. 1992; Su et al. 2007; Ryu et al. 2019; Zhu et al. 2001; Provenzano et al. 2014), no one has conducted a comprehensive high-resolution mapping of this protein in mammalian brain development. In this study, we present a high-resolution, comprehensive map of NF1 expression in the developing mouse brain. Using in situ hybridization and immunohistochemistry (IHC), we characterize the precise spatiotemporal distribution of NF1 across major brain regions and cell lineages from early embryonic stages through

postnatal maturation. Moreover, we used publicly available single-nuclei RNA-seq (snRNA-seq) databases of the adult mouse brain to map NF1 expression across different cell clusters, at a resolution much higher than achievable with classical techniques alone. These results revealed a previously unreported graded expression pattern of NF1.

Results:

NF1 is expressed in different cell lineages of the murine forebrain

Using IHC, we observed broad NF1 expression in different parts of the mouse forebrain, such as the neocortex, hippocampus, choroid plexus, thalamus, and hypothalamus (**Fig. 1A-P**). In the postnatal day (P)35 hypothalamus, NF1 strongly marked the paraventricular nucleus (PVN), suprachiasmatic nucleus (SCN), and supraoptic nucleus (SON), involved in regulating circadian rhythm, neurohormone release and fluid balance. Similar localization of *Nf1* mRNA was also observed at P35 and P0 using *in situ* hybridization (**Supplementary Fig. S1A-B"**). In embryonic ages E17.5, E14.5, and E12.5, NF1 protein expression was observed along the lateral and third ventricular linings, including neocortical and ventral telencephalic ventricular zone, cortical hem, and hippocampal primordium (**Fig. 1D-F**). Specifically, NF1 showed perinuclear expression in the neocortical plate and white matter as well as CA fields and hilus of hippocampus, but not dentate gyrus (DG) (**Fig. 1G-I**). By colabelling with different cell-type-specific telencephalic markers across development, we identified sets of cells that express the NF1 protein (**Fig. 2**). We observed strong perinuclear labelling of NF1 in excitatory pyramidal neocortical neurons from the peak neurogenic stage at E14.5 till developed cortical stage at P35 (**Fig. 2A-H,K,L**). This includes coexpression with markers specific to all mature pyramidal neurons (NeuN), deep layer-specific neurons (Ctip2), and upper layer neurons (Satb2). When checked for colocalization with the progenitors at the neocortical ventricular zone, NF1 was found perinuclearly in the $Sox2^+$ apical progenitors at E17.5, E14.5, and E12.5, but not in the $Tbr2^+$ intermediate progenitor cells (**Fig. 2I,J,M-P**). Further, NF1 was strongly expressed in the hippocampal CA1 and CA3 pyramidal neurons and hilar neurons but did not label any cells in the dentate gyrus (DG), as observed at P35, P0 and E17.5 (**Fig. 2Q-Y"**). These were determined by colabelling NF1 with NeuN to mark all differentiated hippocampal neurons across ages, and Ctip2, which prominently marks CA1 and developing DG at E17.5. Even at E14.5, weak NF1 expression was observed in the ventricular zone of cortical hem and hippocampal primordium/anlage (**Fig. 2Z-Z"**). E12.5 dorsal midline showed mild NF1 expression mostly concentrated along the ventricular lining (**Fig. 2AA-AA"**).

We also observed strong NF1 expression in different subtypes of cortical interneurons at P35, colabelling with Parvalbumin and Somatostatin (**Supplementary Fig. S2A-D"**). Interestingly, NF1 was observed to be present only in certain subsets of $Olig2^+$ oligodendrocyte populations in the major axonal tracts of P35 mouse forebrain, namely corpus callosum, hippocampal commissure, and anterior commissure (**Fig. 3A-F''**). This observation may suggest differential function of molecularly distinct subtypes of oligodendrocytes when NF1 levels are disrupted in the brain.

155
156 **NF1 is expressed in different cell lineages of the murine cerebellum**

157 Unlike the forebrain, a more restricted protein expression profile of NF1 was observed in
158 the murine cerebellum across the developmental timeline (**Fig. 4A-J”**). Particularly,
159 strong perinuclear NF1 expression was observed in mature and migrating Purkinje cells,
160 colabelling with Calbindin (**Fig. 4E’,F’,G’; Fig. 5A-D”**). On the other hand, very low or
161 no IHC signal of NF1 was observed at any stage of cerebellar granule cell development,
162 when colabelled with NeuN (**Fig. 5E-H”,M,N**). *Nf1* mRNA was also observed in the
163 parts of cerebellum at P35 and P0 using *in situ* hybridization (**Supplementary Fig.**
164 **S1C-D”**). Intriguingly, NF1 expression was observed throughout the development of the
165 cerebellar neurons, be it in the migratory state or transitory state at the embryonic
166 nuclear transitory zone (NTZ) or later when forming the deep cerebellar nuclei (DCN)
167 located within the white matter (**Fig. 4E”,F”,G”H”, I,I’,J,J’**). It was coexpressed with
168 NeuN, marking neurons at the DCN, from P3 to P35 (**Fig. 5I-K”**); NeuN+ cells were not
169 present in the prospective DCN area at P0 (**Fig. 5L-L”**).
170
171 At embryonic stages, the cerebellar anlage has distinct proliferative zones, namely
172 rhombic lip and cerebellar ventricular zone (CVZ) (Leto et al. 2016). At early cerebellar
173 development (E12.5), CVZ is further subdivided molecularly into the Purkinje cell-
174 producing zone and the Pax2$^+$ interneuron-producing zone. Later in development, the
175 whole CVZ becomes potent to produce cerebellar interneurons. Perinuclear NF1
176 expression was observed around Sox2+ nuclei in the apical progenitors of the CVZ at
177 E12.5 and E14.5 (**Fig. 6 A-B-B”,D,E-E”**). However, no overlap was observed in
178 rhombic lip-derived Pax6$^+$ cells at E12.5 or E14.5 (**Fig. 6C-C”, F-F”**). We also found
179 NF1 to mark differentiated Pax2$^+$ cells that have migrated out of the interneuron-
180 producing side of the CVZ at E14.5 (**Fig. 4 I,I”, Supplementary Fig. S3A-B”**).
181 However, NF1 was expressed in only a small subset of Tbr2+ rhombic lip-derived
182 unipolar brush cells at E14.5 (**Supplementary Fig. S3E-E”**).
183
184 Finally, similar to forebrain results, NF1 showed an interesting expression pattern in glial
185 lineages of the cerebellum (**Fig. 7A-N”**). At both the cerebellar folium and the DCN
186 region, NF1 showed perinuclear expression in a subset of Olig2$^+$ oligodendrocytes, as
187 observed at P35 and P12 (**Fig. 7A-H”**). The same trend was observed in the
188 subpopulations of Bergmann glia, which are unipolar astrocytes of the cerebellum (**Fig.**
189 **7I-N”**).
190
191 Taken together, here we report differential expression of NF1 in the mouse brain,
192 specifically in glial populations, along development. This suggests the possibility of
193 alternate regulatory mechanisms that eventually govern brain function.
194

195 **NF1 is expressed in distinct cell layers of the eye and olfactory bulb**

196 Beyond regular brain regions, NF1 was also found to be expressed in accessory brain
197 regions like the eye and olfactory bulb, both of which are connected to neurosensation
198 (**Fig. 8A-R"**). Expression of NF1 in the developing eye was substantially strong in the lens,
199 retinal pigmented epithelium (RPE), and neuroretina. In the neuroretina, NF1 expression
200 was distinct in the photoreceptor cell layer (PRC), and in the retinal ganglionic cells and
201 Müller glial cells present in the ganglionic cell layer. A subset of $NF1^+$ cells in the retinal
202 ganglionic cell (RGC) layer colocalized with Tbr2, which is known to be a key regulator of
203 the intrinsically photosensitive RGCs (Chen et al. 2021). $Sox2^+$ zone of E14.5 and E17.5
204 neuroretina largely did not overlap with the $NF1^+$ layers, apart from the PRCs (**Fig. 8A,C-**
205 **F"**). With respect to the developing olfactory bulb, NF1 was observed specifically in the
206 mitral cell layer (MCL) of the main olfactory bulb (MOB), which are projection neurons
207 critical for processing the sense of odours (Davison & Katz 2007). NF1 was also
208 expressed in the accessory olfactory bulb (AOB) from P0 to P35, which is important for
209 aggression and reproduction (Ennis & Holy 2015) (**Fig. 8G-J**). NF1 overlapped with NeuN
210 in the MCL at P35 and P12 (**Fig. 8K,L,O-P''**). On the other hand, it did not have much
211 overlap with $Pax6^+$ cells at P3 and P0, apart from posterior AOB (**Fig. 8M,N,Q-R"**).
212

213 **Reanalysis of single nuclei RNAseq data reveals enriched *Nf1* expression in**
214 **diverse neural cell types**

215 To determine the expression of *Nf1* at higher resolution, we utilized publicly available
216 single-nuclei RNAseq databases (Mortberg et al. 2023; Kozareva et al. 2021). In the
217 adult mouse cortex, *Nf1* expression was identified in almost all the marked cortical
218 clusters (**Fig. 9A-C**). However, detailed analysis revealed specific enrichment of *Nf1*
219 transcripts in the lineages of cortical interneurons, oligodendrocytes, and excitatory
220 neurons (**Fig. 9D**). In particular, *Nf1* expression was found to be highest in the
221 oligodendrocyte lineage. Moreover, among different oligodendrocyte clusters, *Nf1*
222 expression was found to be highest in differentiating oligodendrocytes (**Fig. 9D**). Based
223 on our IHC data, all Olig2+ cells in the cortex were not positive for NF1. Hence, we
224 looked at the percentage of cells positive for *Nf1* expression across different cortical
225 clusters (**Fig. 9E**). Interestingly, oligodendrocyte precursor cells (OPCs) and
226 differentiating OPCs showed a very high frequency of *Nf1*-expressing cells than mature
227 oligodendrocytes. This data strongly suggests the importance of NF1 in oligodendrocyte
228 development. Besides oligodendrocytes, cortical interneurons and excitatory pyramidal
229 neurons also exhibit higher frequency and expression, corroborating our IHC findings.
230

231 We performed a similar analysis on adult cerebellum and identified an enriched
232 expression of *Nf1* in CVZ-derivatives, such as cerebellar interneurons, Purkinje cells,
233 Bergmann glia, and rhombic lip-derivative unipolar brush cell (**Fig. 9F-H**). Among these

clusters, the highest expression was found in the Bergmann glial cells (**Fig. 9I**). Similarly, *Nf1* showed enriched expression in the oligodendrocyte lineage of the adult neocortex, with a higher frequency of *Nf1*-expressing cells in the OPC cluster as compared to mature oligodendrocytes (**Fig. 9H**). The frequency plot also demonstrated that almost all cells in the Purkinje cell cluster were positive for *Nf1*, thus aligning with our IHC expression data.

Overall, these reanalysis results not only validated our IHC data but also helped identify *Nf1* expression in some neural cell types, such as differentiating oligodendrocytes, which are difficult to capture using conventional IHCs. Our in-depth analysis also uncovered the graded expression pattern of *Nf1* across diverse cell types in the murine adult brain. This may suggest the differential role of *Nf1* in these diverse subtypes.

Discussion:

In this comprehensive study, we demonstrate the spatiotemporal expression of neurofibromin (NF1) in the murine brain across embryonic, perinatal, and adult developmental time points, using IHC, *in situ* hybridization, and reanalyses of publicly available single-nuclei RNA-seq datasets. To our knowledge, this is the first report of an NF1 expression study, not only across major brain regions but also along almost the entire span of development. Crucially, our findings reveal molecularly distinct neural subtypes in the forebrain and cerebellum defined by the presence or absence of NF1, suggesting a previously unappreciated heterogeneity in NF1-mediated signaling during neurodevelopment. The high degree of concordance between our protein (IHC) and transcriptomic (snRNA-seq) data establishes a robust framework for understanding the role of NF1 in neural development.

Cell-type-specific NF1 expression in the forebrain suggests roles in neuronal lineage progression and excitation-inhibition balance

In this study, we identify broad yet cell-type-specific NF1 expression across the developing and postnatal forebrain, including the neocortex, hippocampus, and major white matter tracts. NF1 demonstrated consistent perinuclear localization and strong agreement between protein and transcript levels. In the neocortex, it is expressed in excitatory pyramidal neurons across all layers and in Sox2^{+} apical progenitors, but interestingly not in Tbr2^{+} intermediate progenitors. This indicates a stage-specific role of NF1 during cortical neurogenesis. In parallel, NF1 is expressed in inhibitory interneurons, including Parvalbumin^{+} and Somatostatin^{+} populations. This suggests that NF1 is involved in both arms of cortical circuitry, raising the possibility that NF1 loss can disrupt excitation–inhibition balance. In the hippocampus, NF1 shows region-specific enrichment in the pyramidal neurons of CA fields and hilar neurons, but is notably absent from the dentate gyrus, suggesting subfield-specific functional roles. Besides, its expression is also observed in specific hypothalamic and thalamic nuclei of the diencephalon, as well as in the ventricular zone of the ventral telencephalon in younger ages. Together, these findings position NF1 as a key regulator across multiple forebrain cell types, with potential implications for lineage specification, neuronal integrity, circuit formation, and function.

Role of NF1 in cerebellar development and motor coordination

In the cerebellum, NF1 is expressed across multiple neuronal populations throughout development, including deep cerebellar nuclei (DCN) neurons, Purkinje neurons, and cerebellar interneurons across all examined stages. In the cerebellum, proper functioning of DCN neurons and associated circuits is critical for having regular motor coordination and function (Lackey et al. 2023; van der Heijden 2024). The persistent expression of NF1 identified in the DCN and developing neurons throughout our

experimental timeline highlights its importance in motor circuits. Mutations in *NF1* may impair the development or function of these neurons, resulting in motor deficits, as commonly seen in patients harbouring *NF1* mutations (Rietman et al. 2017). Similarly, defects in NF1 may affect the Purkinje cell- and cerebellar interneuron-related miscoordination. We also observed NF1 expression in subsets of Bergmann glia, cerebellar astrocytic cells that coordinate cell-cell communication, support development, and prevent neurological injury (Araujo et al. 2019; De Zeeuw & Hoogland 2015; Buffo & Rossi 2013). Having the knowledge of which subtype is affected in a disease condition may help identify specific therapeutic interventions.

Mosaic NF1 expression across neural lineages reveals previously unrecognized cellular heterogeneity

Our analyses reveal molecular heterogeneity within both neuronal and glial populations based on NF1 expression status, identifying NF1+ve and NF1−ve subpopulations across brain regions and suggesting a mosaic pattern of expression. In particular, distinct NF1+ve and NF1−ve subsets of Olig2^{+} oligodendrocytes are observed in cerebellum and major forebrain white matter tracts, while only a subset of Bergmann glia expresses NF1. This reveals previously unappreciated diversity within glial lineages. These findings are supported both by IHC data and snRNA-seq analyses. In addition, transcriptomic data reveal NF1+ve and NF1−ve interneuron populations in the cortex and cerebellum, extending this heterogeneity to neuronal lineages. The functional significance of this differential expression remains unclear, but it suggests several possibilities: NF1 may mark distinct developmental trajectories, reflect differences in maturation state, or be dynamically regulated within lineages, defining transient cellular states. These observations raise key questions regarding the developmental origins of NF1+ve and NF1−ve populations, the mechanisms controlling NF1 expression, and the functional consequences of this heterogeneity, which may ultimately contribute to variability in NF1-associated disease phenotypes.

NF1 expression in sensory systems extends its role to photo-dependent and olfactory circuitry

Beyond the major regions of the brain, we report NF1 expression also in specific layers of the developing eye and olfactory bulb, offering new insights into sensory-related pathologies. Specifically, NF1 is expressed in the photoreceptor layer of the neuroretina, which is vital for visual phototransduction (Hussey et al. 2022). It is also identified in Müller glial cells, which provide support and guidance for the light to reach the photoreceptor layer (Franze et al. 2007), and retinal ganglion cells (RGCs), which finally transmit sensory information to the brain. The signal perceived by the eye is known to produce both visual and non-visual responses in different parts of the diencephalon (Peirson et al. 2018). While light information cascades through the

thalamic nuclei to the visual cortex for vision, it also triggers the hypothalamic nuclei critical for circadian rhythm, sleep and neuroendocrine functions (Dumbell et al. 2016; Trachtman 2010). Our study revealed NF1 expression specifically in the SCN, the master circadian rhythm generator, and in the VPN and SON, neuroendocrine nuclei involved in fluid balance and rhythmic production of hormones. Together, these strongly suggest a potential role of NF1 in light sensation, transduction, and eventually the light-dependent regulatory functions in the brain. Further work may reveal novel molecular interactions between NF1 and the diencephalon regulating sleep and metabolic homeostasis.

Similarly, the presence of NF1 expression in the mitral cells of the olfactory bulb and in both parts of the AOB suggests an underexplored role for NF1 in odor and pheromone processing and in pheromone-driven behaviors, such as reproductive and defensive responses. The conservation of these patterns suggests that NF1 may be integral to evolutionary ancient sensory circuits.

Implications for NF1-associated neurodevelopmental disorders and tumorigenesis

This comprehensive atlas of NF1 expression across murine brain development provides a framework for linking cellular context to NF1-associated neurodevelopmental disorders and tumorigenesis. The widespread yet heterogeneous expression of NF1 across neuronal and glial populations suggests that its dysregulation may impact multiple circuits and developmental processes, contributing to the clinical variability observed in NF1 patients. The identification of NF1+ve and NF1−ve subpopulations further raises the possibility of selective cellular vulnerability, which may influence both disease manifestation and tumor initiation. These findings offer a basis for identifying cells of origin and critical developmental windows in NF1-associated pathologies.

Overall, this work provides a resource for understanding NF1 function in the developing brain and supports future efforts toward cell-type-specific and targeted therapeutic strategies.

Limitations of the study

While this study provides a comprehensive spatiotemporal map of NF1 expression, several limitations should be considered. First, our analyses are primarily descriptive and based on IHCs, *in situ* hybridization, and reanalysis of existing snRNAseq datasets; therefore, they do not directly address the functional consequences of NF1 loss in specific cell types. Second, although strong concordance is observed across modalities, differences in sensitivity and resolution between protein- and transcript-level measurements may influence the detection of low-abundance or transient expression of

NF1 in different cellular lineages. In addition, our conclusions are drawn from murine models, and although broadly informative, species-specific differences may limit direct translation to human biology. The observed NF1+ve and NF1−ve heterogeneity across cell populations also remains unresolved, particularly with respect to developmental origin, temporal dynamics, and regulatory mechanisms. Addressing these limitations through functional perturbation studies, higher-resolution temporal analyses, and cross-species validation will be important for further elucidating the role of NF1 in brain development and disease.

376 **Materials and methods:**
377
378 **Key resources table:**
379

Reagent type/ resource	Designation	Reference/ Source	Identifiers
Mouse	FVB/NJ	Gift from Prof Kathleen Millen, Seattle Children's Research Institute, USA	-
Antibody	Anti-Parvalbumin Antibody	Merck	Millipore (Cat # MAB1572, RRID:AB_2174013)
Antibody	Anti-Somatostatin Antibody, clone YC7	Merck	Sigma-Aldrich (Cat # MAB354, RRID: AB_2255365)
Antibody	Calbindin D28K Monoclonal Antibody (5A9)	Thermo Fisher Scientific	Invitrogen (Cat # MA5-47441, RRID:AB_2942423)
Antibody	SOX2 Monoclonal Antibody (20G5)	Thermo Fisher Scientific	Invitrogen (Cat # MA1-014, RRID:AB_2536667)
Antibody	Ki-67 Monoclonal Antibody (SolA15)	Thermo Fisher Scientific	Invitrogen (Cat # 14-5698-82, RRID:AB_10854564)
Antibody	Olig2 (F9R1H) Mouse Monoclonal Antibody	Cell Signaling Technology	CellSignalingTechnology (Cat # 39588)
Antibody	PAX2 Monoclonal Antibody (3C7)	Thermo Fisher Scientific	Invitrogen (Cat # H00005076-M01)
Antibody	PAX6 Monoclonal Antibody (GT9412)	Thermo Fisher Scientific	Invitrogen (Cat # MA5-50298, RRID:AB_3094028)
Antibody	Anti-NeuN Antibody, clone A60	Merck	Sigma-Aldrich (Cat # MAB377, RRID: AB_2298772)
Antibody	ALDH1L1 mouse monoclonal antibody, clone UMAB43	OriGene	Origene (Cat # UM500039, RRID:AB_2629053)
Antibody	Anti-Iba1 goat polyclonal antibody	Abcam	Abcam (Cat # ab5076, RRID:AB_2224402)
Antibody	Custom Rabbit polyclonal antibody	Neurodevelopment lab, India	

	against NF1		
Antibody	Anti-SATB1 + SATB2 antibody [SATBA4B10] - C-terminal	Abcam	Abcam (Cat # ab51502, RRID:AB_882455)
Antibody	Anti-Ctip2 antibody [25B6]	Abcam	Abcam (Cat # ab18465, RRID:AB_2064130)
Antibody	Anti-Tbr1 Antibody	Merck	Millipore (Ca t# AB2261, RRID:AB_10615497)
Antibody	EOMES Monoclonal Antibody (Dan11mag)	Thermo Fisher Scientific	Invitrogen (Cat # 14-4875-82, RRID:AB_11042577)
Antibody	FOXJ1 Monoclonal Antibody (2A5)	Thermo Fisher Scientific	Invitrogen (Cat # 14-9965-82, RRID:AB_1548835)
Antibody	Goat anti-Mouse IgG (H+L) Highly Cross-Adsorbed Secondary Antibody, Alexa Fluor™ 488 -	Thermo Fisher Scientific	Invitrogen (Cat # A-11029, RRID:AB_2534088)
Antibody	Goat anti-Rabbit IgG (H+L) Highly Cross-Adsorbed Secondary Antibody, Alexa Fluor™ 568 -	Thermo Fisher Scientific	Invitrogen (Cat # A-11036, RRID:AB_10563566)
Antibody	Goat anti-Rat IgG (H+L) Cross-Adsorbed Secondary Antibody, Alexa Fluor™ 647	Thermo Fisher Scientific	Invitrogen (Cat # A-21247, RRID:AB_141778)
Antibody	Goat anti-Chicken IgY (H+L) Secondary Antibody, Alexa Fluor™ 568	Thermo Fisher Scientific	Invitrogen (Cat # A-11041, RRID:AB_2534098)
Antibody	Goat anti-Rabbit IgG (H+L) Highly Cross-Adsorbed Secondary Antibody, Alexa Fluor™ 488	Thermo Fisher Scientific	Invitrogen (Cat # A-11034, RRID:AB_2576217)
Antibody	Donkey anti-Goat IgG (H+L) Cross-Adsorbed Secondary	Thermo Fisher Scientific	Invitrogen (Cat # A-21447, RRID:AB_2535864)

	Antibody, Alexa Fluor™ 647		
Commercial assay/Kit	RNAscope™ 2.5 HD Reagent Kit-RED	Biotechne	ACD (Cat # 322350)
Probe	RNAscope™ Negative Control Probe	Biotechne	ACD (Cat # 320751)
Probe	RNAscope™ Positive Control Probe- Mm-Polr2a	Biotechne	ACD (Cat # 312471)
Probe	RNAscope Probe Mm Nf1 C1	Biotechne	ACD (Cat # 417351)
Software, Algorithm	Fiji	PMID: 22743772	
Software, Algorithm	10x Genomics Cell Ranger v10.0.0		Single-cell analyses
Software, Algorithm	Seurat v5	PMID: 37231261	Single-cell analyses

Mice:

For all the experiments FVB/NjJ mouse strain was used. Mice were housed and bred under pathogen-free conditions in the animal facility at Jawaharlal Nehru Centre for Advanced Scientific Research (JNCASR, India). All mice received food and water *ad libitum* and were subjected to a 12-hour light-dark cycle. Noon of the day of vaginal plug was designated as embryonic day 0.5 (E0.5). The day of birth was designated as postnatal day 0 (P0), which usually occurs between E19-20.

Sample preparation:

Brains from postnatal pups were harvested in phosphate buffer saline (PBS), then were fixed in 10% Formalin Solution neutral buffer (10% NBF) for 48-72 hrs for P35 and 2-6hrs for all embryonic and early postnatal ages, equilibrated in 30% (wt/vol) sucrose made in 1X PBS, and sectioned at 30 µm on a freezing microtome (Leica, Germany). These sections were then processed for *in situ* hybridization or immunohistochemical procedures.

Immunohistochemistry:

boiled in 10mM sodium citrate solution for antigen retrieval, blocked in 10% serum in PBS with 0.1% Triton X-100, and then incubated for 36-48hrs at 4°C with primary antibodies. The next day, sections were washed thrice in PBS, incubated with

401 appropriate species-specific secondary antibodies conjugated with Alexa 488, 568, or
402 647 fluorophores (Invitrogen) for 2 hrs at room temperature and then counterstained
403 with 4′,6-diamidino-2-phenylindole (DAPI) to visualize the nuclei. Sections were
404 coverslipped using Fluoromount G mounting medium (Fisher Scientific, USA).
405 Information regarding the antibodies used in this study is listed in the Key Resources
406 table above. Immunohistochemistry experiments were replicated with biologically
407 independent samples (minimum three). All attempts for replication were successful. No
408 outliers were encountered. Each antibody was validated for mouse and application
409 (IHC) by the respective manufacturer, and the data are publicly available. This was also
410 validated by us in our experiments, replicating published/expected expressions in
411 control tissue.
412
413 ***In situ* hybridization:**
414 Assays were run using commercially available probes from Advanced Cell Diagnostics
415 (ACD, Biotechne). Manufacturer-recommended protocols were used without
416 modification. Sections were probed using *Nf1* (Cat# 417351) and counterstained with
417 hematoxylin.
418
419 **Imaging of brain sections:**
420 Imaging of IHC brain sections was done using CellVoyager™ CQ1 Benchtop High-
421 Content Analysis System using CellPathfinder (Yokogawa, Japan), and later processed
422 in ImageJ software (NIH, Bethesda, Maryland, USA). *In situ* slides were visualized
423 under an Olympus VS 200 slide scanner brightfield microscope. Apart from minor
424 adjustments to contrast and brightness across the entire image, there was no further
425 image alteration. Pseudo-colouring was used to highlight the cells of interest. Figures
426 were prepared on Adobe Illustrator.
427
428 **Reanalysis of single-nuclei transcriptomics datasets:**
429 Using Single Cell Portal (singlecell.broadinstitute.org/single_cell), we conducted a
430 reanalysis of single-nuclei RNAseq data of adult cerebellum (SCP795) and adult cortex
431 (SCP2126), originally reported by (Mortberg et al. 2023) and (Kozareva et al. 2021),
432 respectively. The Seurat object was downloaded from the portal, and downstream
433 analysis was performed using Seurat v5 (Hao et al. 2024). UMAP clusters were
434 annotated to different neural cell types based on their transcriptomic signatures. We
435 specifically focused on examining Nf1 expression levels across diverse cell types.
436 Subsequently, we generated graphical plots with the help of ggplot2 package (Wickham
437 2016).
438

Author Contributions:
VL and AR contributed to the study conception, study design, data acquisition, data analysis, and interpretation. VL and AR wrote the first draft of the manuscript, reviewed it, and approved the final version. AR provided funding and infrastructural resources.

Acknowledgements:
We thank Prof Kathleen J Millen, Seattle Children's Research Institute, for gifting the FVB mouse line; Varun M. and Shruti Srivastava for technical support during image acquisition. Cerebellar lamination schematics in Fig. 5M and 5N have been created using the BioRender software (https://www.biorender.com/).

Funding:
This work was funded by the Ramalingaswami Re-entry Fellowship (BT/RLF/Re-entry/73/2020) from the Department of Biotechnology (DBT), India (AR); the Prime Minister Early Career research Grant (PM-ECRG, ANRF/ECRG/2024/001273/LS) from the Anusandhan National Research Foundation (ANRF), India (AR); Early Career Award from the International Brain Research Organization (IBRO, ECA-8126694738) (AR); and the intramural funding from the Jawaharlal Nehru Centre for Advanced Scientific Research, India (AR).

Ethics
Animal experimentation: All animal experimentation was conducted in accordance with the guidelines laid down by the Institutional Animal Ethics Committees (IAEC) of Jawaharlal Nehru Centre for Advanced Scientific Research, India (protocols AR 002 and AR 003).

Data/resource availability:
All relevant data and details on resources are provided in the article and its supplementary information.

Conflict of interest:
The authors declare that the research was conducted in the absence of any commercial or financial relationships that could be construed as a potential conflict of interest.

Diversity and inclusion statement
Preparation of this document has involved diversity and inclusion practices relevant to both the scientific content of the paper and authorship and attribution.

476 **References:**

477 Albers, A.C. & Gutmann, D.H., 2009. Gliomas in patients with neurofibromatosis type 1. *Expert*
478 *Review of Neurotherapeutics*, 9(4), pp.535–539. Available at:
479 https://doi.org/10.1586/ern.09.4.

480 Araujo, A.P.B., Carpi-Santos, R. & Gomes, F.C.A., 2019. The role of astrocytes in the
481 development of the cerebellum. *Cerebellum (London, England)*, 18(6), pp.1017–1035.
482 Available at: https://doi.org/10.1007/s12311-019-01046-0.

483 Ayasa, L.A. et al., 2024. Glioblastoma multiforme in a patient with neurofibromatosis type 1: a
484 case report and review of literature. *Journal of Surgical Case Reports*, 2024(8), p.rjae517.
485 Available at: https://doi.org/10.1093/jscr/rjae517.

486 Báez-Flores, J., Rodríguez-Martín, M. & Lacal, J., 2023. The therapeutic potential of
487 neurofibromin signaling pathways and binding partners. *Communications Biology*, 6(1),
488 p.436. Available at: http://dx.doi.org/10.1038/s42003-023-04815-0.

489 Balestri, P. et al., 2003. Malformations of cortical development in neurofibromatosis type 1.
490 *Neurology*, 61(12), pp.1799–1801. Available at:
491 https://doi.org/10.1212/01.WNL.0000099080.90726.BA.

492 Brannan, C.I. et al., 1994. Targeted disruption of the neurofibromatosis type-1 gene leads to
493 developmental abnormalities in heart and various neural crest-derived tissues. *Genes &*
494 *Development*, 8(9), pp.1019–1029. Available at: http://dx.doi.org/10.1101/gad.8.9.1019.

495 Buffo, A. & Rossi, F., 2013. Origin, lineage and function of cerebellar glia. *Progress in*
496 *Neurobiology*, 109, pp.42–63. Available at: https://doi.org/10.1016/j.pneurobio.2013.08.001.

497 Chen, C.-K. et al., 2021. Characterization of Tbr2-expressing retinal ganglion cells. *The Journal*
498 *of Comparative Neurology*, 529(15), pp.3513–3532. Available at:
499 http://dx.doi.org/10.1002/cne.25208.

500 Cichowski, K. & Jacks, T., 2001. NF1 tumor suppressor gene function: narrowing the GAP. *Cell*,
501 104(4), pp.593–604. Available at: http://dx.doi.org/10.1016/s0092-8674(01)00245-8.

502 Daston, M.M. et al., 1992. The protein product of the neurofibromatosis type 1 gene is
503 expressed at highest abundance in neurons, Schwann cells, and oligodendrocytes. *Neuron*,
504 8(3), pp.415–428. Available at: https://doi.org/10.1016/0896-6273(92)90270-N.

505 Davison, I.G. & Katz, L.C., 2007. Sparse and selective odor coding by mitral/tufted neurons in
506 the main olfactory bulb. *The Journal of Neuroscience: The Official Journal of the Society for*
507 *Neuroscience*, 27(8), pp.2091–2101. Available at:
508 https://doi.org/10.1523/JNEUROSCI.3779-06.2007.

509 De Zeeuw, C.I. & Hoogland, T.M., 2015. Reappraisal of Bergmann glial cells as modulators of
510 cerebellar circuit function. *Frontiers in Cellular Neuroscience*, 9, p.246. Available at:
511 https://doi.org/10.3389/fncel.2015.00246.

512 Dumbell, R., Matveeva, O. & Oster, H., 2016. Circadian clocks, stress, and immunity. *Frontiers*
513 *in Endocrinology*, 7, p.37. Available at: http://dx.doi.org/10.3389/fendo.2016.00037.

514 Durkin, J. et al., 2023. Neurofibromin 1 regulates early developmental sleep in Drosophila.
515 *Neurobiology of Sleep and Circadian Rhythms*, 15(100101), p.100101. Available at:
516 http://dx.doi.org/10.1016/j.nbscr.2023.100101.

517 Ennis, M. & Holy, T.E., 2015. Anatomy and neurobiology of the main and accessory olfactory
518 bulbs. *Handbook of Olfaction and Gustation*, pp.157–182. Available at:
519 http://dx.doi.org/10.1002/9781118971758.ch8.

520 Franze, K. et al., 2007. Müller cells are living optical fibers in the vertebrate retina. *Proceedings*
521 *of the National Academy of Sciences of the United States of America*, 104(20), pp.8287–
522 8292. Available at: http://dx.doi.org/10.1073/pnas.0611180104.

523 Gutmann, D.H. et al., 1999. Haploinsufficiency for the neurofibromatosis 1 (NF1) tumor
524 suppressor results in increased astrocyte proliferation. *Oncogene*, 18(31), pp.4450–4459.
525 Available at: https://doi.org/10.1038/sj.onc.1202829.

526 Hao, Y. et al., 2024. Dictionary learning for integrative, multimodal and scalable single-cell
527 analysis. *Nature Biotechnology*, 42(2), pp.293–304. Available at:
528 https://doi.org/10.1038/s41587-023-01767-y.

529 van der Heijden, M.E., 2024. Converging and diverging cerebellar pathways for motor and
530 social behaviors in mice. *Cerebellum (London, England)*, 23(5), pp.1754–1767. Available
531 at: http://dx.doi.org/10.1007/s12311-024-01706-w.

532 Hussey, K.A., Hadyniak, S.E. & Johnston, R.J., Jr, 2022. Patterning and development of
533 photoreceptors in the human retina. *Frontiers in Cell and Developmental Biology*, 10,
534 p.878350. Available at: http://dx.doi.org/10.3389/fcell.2022.878350.

535 Hyman, S.L., Shores, A. & North, K.N., 2005. The nature and frequency of cognitive deficits in
536 children with neurofibromatosis type 1. *Neurology*, 65(7), pp.1037–1044. Available at:
537 https://doi.org/10.1212/01.wnl.0000179303.72345.ce.

538 Jacks, T. et al., 1994. Tumour predisposition in mice heterozygous for a targeted mutation in
539 Nf1. *Nature Genetics*, 7(3), pp.353–361. Available at: https://doi.org/10.1038/ng0794-353.

540 Karaconji, T. et al., 2019. Neurofibromatosis type 1: Review and update on emerging therapies.
541 *Asia-Pacific Journal of Ophthalmology (Philadelphia, Pa.)*, 8(1), pp.62–72. Available at:
542 http://dx.doi.org/10.22608/APO.2018182.

543 Kozareva, V. et al., 2021. A transcriptomic atlas of mouse cerebellar cortex comprehensively
544 defines cell types. *Nature*, 598(7879), pp.214–219. Available at:
545 https://doi.org/10.1038/s41586-021-03220-z.

546 Lackey, E.P., Rey Hipolito, A.G. & Sillitoe, R.V., 2023. Motor circuit abnormalities during
547 cerebellar development. In *Contemporary Clinical Neuroscience*. Cham: Springer
548 International Publishing, pp. 129–154. Available at: http://dx.doi.org/10.1007/978-3-031-
549 23104-9_7.

550 Lakkis, M.M. et al., 1999. Neurofibromin deficiency in mice causes exencephaly and is a
551 modifier for Splotch neural tube defects. *Developmental Biology*, 212(1), pp.80–92.
552 Available at: https://doi.org/10.1006/dbio.1999.9327.

553 Leto, K. et al., 2016. Consensus paper: Cerebellar development. *Cerebellum (London,*
554 *England)*, 15(6), pp.789–828. Available at: http://dx.doi.org/10.1007/s12311-015-0724-2.

555 Lolam, V. & Roy, A., 2025. Developmental mechanisms underlying pediatric epilepsy. *Frontiers*
556 *in Neurology*, 16, p.1586947. Available at: http://dx.doi.org/10.3389/fneur.2025.1586947.

557 Lucas, C.-H.G. et al., 2022. Multiplatform molecular analyses refine classification of gliomas
558 arising in patients with neurofibromatosis type 1. *Acta neuropathologica*, 144(4), pp.747–
559 765. Available at: https://doi.org/10.1007/s00401-022-02478-5.

560 Martin, G.A. et al., 1990. The GAP-related domain of the neurofibromatosis type 1 gene product
561 interacts with ras p21. *Cell*, 63(4), pp.843–849. Available at: http://dx.doi.org/10.1016/0092-
562 8674(90)90150-d.

563 Mortberg, M.A. et al., 2023. A single-cell map of antisense oligonucleotide activity in the brain.
564 *Nucleic Acids Research*, 51(14), pp.7109–7124. Available at:
565 https://doi.org/10.1093/nar/gkad371.

566 Nix, J.S., Blakeley, J. & Rodriguez, F.J., 2020. An update on the central nervous system
567 manifestations of neurofibromatosis type 1. *Acta neuropathologica*, 139(4), pp.625–641.
568 Available at: http://dx.doi.org/10.1007/s00401-019-02002-2.

569 Peirson, S.N. et al., 2018. Light and the laboratory mouse. *Journal of Neuroscience Methods*,
570 300, pp.26–36. Available at: https://doi.org/10.1016/j.jneumeth.2017.04.007.

571 Plasschaert, E. et al., 2015. Prevalence of Autism Spectrum Disorder symptoms in children with
572 neurofibromatosis type 1. *American Journal of Medical Genetics. Part B, Neuropsychiatric*
573 *Genetics: The Official Publication of the International Society of Psychiatric Genetics*,
574 168B(1), pp.72–80. Available at: http://dx.doi.org/10.1002/ajmg.b.32280.

575 Provenzano, G. et al., 2014. Hippocampal dysregulation of neurofibromin-dependent pathways
576 is associated with impaired spatial learning in engrailed 2 knock-out mice. *The Journal of*
577 *Neuroscience: The Official Journal of the Society for Neuroscience*, 34(40), pp.13281–
578 13288. Available at: http://dx.doi.org/10.1523/JNEUROSCI.2894-13.2014.

579 Rietman, A.B. et al., 2017. Motor problems in children with neurofibromatosis type 1. *Journal of*
580 *Neurodevelopmental Disorders*, 9(1), p.19. Available at: http://dx.doi.org/10.1186/s11689-
581 017-9198-5.

582 Roth, J., Ber, R. & Constantini, S., 2019. Neurofibromatosis type 1-related hydrocephalus:
583 Treatment options and considerations. *World Neurosurgery*, 128, pp.e664–e668. Available
584 at: https://doi.org/10.1016/j.wneu.2019.04.231.

585 Ryu, H.-H. et al., 2019. Enriched expression of NF1 in inhibitory neurons in both mouse and
586 human brain. *Molecular Brain*, 12(1), p.60. Available at: https://doi.org/10.1186/s13041-
587 019-0481-0.

588 Sanchez-Ortiz, E. et al., 2014. NF1 regulation of RAS/ERK signaling is required for appropriate
589 granule neuron progenitor expansion and migration in cerebellar development. *Genes &*
590 *Development*, 28(21), pp.2407–2420. Available at:
591 http://dx.doi.org/10.1101/gad.246603.114.

592 Shin, J. et al., 2012. Zebrafish neurofibromatosis type 1 genes have redundant functions in
593 tumorigenesis and embryonic development. *Disease Models & Mechanisms*, 5(6), pp.881–
594 894. Available at: http://dx.doi.org/10.1242/dmm.009779.

595 Sorrentino, U. et al., 2021. Epilepsy in NF1: Epidemiologic, genetic, and clinical features. A
596 monocentric retrospective study in a cohort of 784 patients. *Cancers*, 13(24), p.6336.
597 Available at: http://dx.doi.org/10.3390/cancers13246336.

598 Su, W. et al., 2007. Mice with GFAP-targeted loss of neurofibromin demonstrate increased
599 axonal MET expression with aging. *Glia*, 55(7), pp.723–733. Available at:
600 http://dx.doi.org/10.1002/glia.20501.

601 Trachtman, J.N., 2010. Vision and the hypothalamus. *Optometry (St. Louis, Mo.)*, 81(2),
602 pp.100–115. Available at: http://dx.doi.org/10.1016/j.optm.2009.07.016.

603 Wickham, H., 2016. Data Analysis. In *Use R!*. Cham: Springer International Publishing, pp. 189–
604 201. Available at: https://doi.org/10.1007/978-3-319-24277-4_9.

605 Zhu, Y. et al., 2001. Ablation of NF1 function in neurons induces abnormal development of
606 cerebral cortex and reactive gliosis in the brain. *Genes & Development*, 15(7), pp.859–876.
607 Available at: http://dx.doi.org/10.1101/gad.862101.

608
609

610 **Figure legends:**
611
612 **Figure 1: NF1 is expressed in mouse forebrain**
613 (A) Schematics showing representative coronal sections of the mouse forebrain at adult
614 and embryonic stages. NF1 protein expression in whole brain (B-E), hippocampus (E-I),
615 and neocortex (J-M) across descending ages P35, P0, E17.5, E14.5, and E12.5. (B-F)
616 NF1 was expressed in distinct zones of thalamus (t) and hypothalamus (hy) in the
617 diencephalon. In the hypothalamus, NF1 clearly marked the paraventricular nucleus
618 (PVN), suprachiasmatic nucleus (SCN), and supraoptic nucleus (SON) (B). Dotted
619 boxes in (B-E) mark insets of parts of telencephalon, namely the neocortex (nctx) and
620 hippocampus (h). (G-I) NF1 expression was observed in CA1, CA3, and hilar cells of
621 hippocampus at E17.5, P0, and P35, but not in the dentate gyrus (DG). (J-K) NF1 was
622 also expressed along the lateral and third ventricular linings, encompassing midline
623 structures, namely choroid plexus (cp), cortical hem (ch), hippocampal primordium (hp),
624 and ventral telencephalon (vtel) across ages (arrows, H-K). (L-P) NF1 is strongly
625 expressed in all mature pyramidal neurons perinuclearly and in the
626 ventricular/subventricular progenitor zones of neocortex across development. P,
627 posterior; A, anterior; hp, hippocampal primordium; cc, corpus callosum; wm, white
628 matter; 3V, third ventricle; lv, lateral ventricle; mz, marginal zone; cp, cortical plate; sp,
629 subplate layer; iz, intermediate zone; vz, ventricular zone; svz, subventricular zone.
630 Scalebars: 500μm (B-F); 100μm (G-K); 50μm (L-P).
631
632 **Figure 2: NF1 colocalizes with mature neurons and apical progenitors of forebrain**
633 (A-D'') NF1 colocalizes with mature neuronal marker NeuN in P35 (A-A'') and P0 (C-C'')
634 neocortical plates (cp); insets show colocalizations indicated as yellow in both ages (B-
635 B'', D-D''). (E-H) NF1 was expressed in both deep and upper neocortical layers.
636 Perinuclear NF1 expression surrounded the nuclear expression of transcription factors
637 Ctip2 and Satb2, respectively demarcating deep and upper layers. (I,J) NF1 is present
638 perinuclearly in $Sox2^+$ apical progenitors at the ventricular zone (vz) but not in $Tbr2^+$
639 intermediate progenitor cells. (K-N) NF1 was expressed in both the developing cortical
640 plate marked by Ctip2 and $Sox2^+$ apical progenitor zone at E14.5, but not in the $Tbr2^+$
641 subventricular zone (svz). (O,P) NF1 was expressed in the $Sox2^+$ apical progenitor zone
642 at E12.5. Arrows in J,N,P indicate perinuclear NF1 expression in the apical progenitors.
643 (Q-Y'') NF1 was expressed predominantly in the CA fields (CA1, CA3) and hilus of P35,
644 P0, and E17.5 hippocampi, but no or low expression was seen in the granular neurons
645 of dentate gyrus (DG) across ages. Hippocampal neuron-dense regions were denoted
646 by NeuN and Ctip2 expression. (Z-AA'') At E14.5 and E12.5, the dorsal midline of the
647 telencephalon showed NF1 expression in choroid plexus (cp), ventricular lining, and a
648 subset of mature neurons derived from the cortical hem (ch) and the hippocampal
649 primordium (hp). nctx, neocortex; wm, white matter; 3V, third ventricle; LV, lateral

650 ventricle; mz, marginal zone; cp, cortical plate; sp, subplate layer; iz, intermediate zone;
651 vz, ventricular zone; h, hippocampus. Scalebars: 100μm (Q-Q'', T-T'', W-W''); 50μm (A-
652 A'', R-S'', U-V''); 25μm (B-C", E-I, K,M,O, X-AA''); 12.5μm (D-D'', F,H,J, L,N,P).
653
654 **Figure 3: NF1 is expressed in subsets of cortical oligodendrocytes**
655 (A-A'') NF1 was expressed in a subset of Olig2$^+$ oligodendrocytes in the main three
656 cortical commissures of the P35 mouse brain - corpus callosum (A-B''), anterior
657 commissure (C-D''), and hippocampal commissure (E-F''). In a magnified view, cream
658 dashed circles mark NF1$^+$Olig2$^+$ double-positive oligodendrocytes, while red dotted
659 circles mark Olig2$^+$ oligodendrocytes that did not express NF1 (B-B", D-D", F-F").
660 Scalebars: 50μm (A-A'', C-C'', E-E''); 25μm (B-B'', D-D'', F-F'').
661
662 **Figure 4: NF1 is expressed in the mouse cerebellum**
663 (A-D) Schematics showing sagittal sections of the mouse forebrain at adult, early
664 postnatal, and embryonic stages, demonstrating how a complex lobular laminated
665 structure like the cerebellum develops from a simple fate-specified neuroepithelium.
666 Boxes mark insets at P35, P12, P3 and P0 indicating magnified views of folium and
667 cerebellar ventricular zone. (E-F'') P35 and P12 cerebella showed strong NF1
668 expression in the Purkinje cell layer (pcl), cells in the white matter (wm), and in the deep
669 cerebellar nuclei (DCN). (G-H'') NF1 was also expressed in migrating Purkinje cells and
670 in developing DCN at perinatal ages, P3 and P0. (I-J"") At E14.5 and E12.5, NF1 was
671 expressed very strongly in immature cerebellar neurons of the nuclear transitory zone
672 (NTZ), and in differentiating neurons near the cerebellar ventricular zone (cvz) and/or
673 extra cerebellar ventricular zone. NF1 was also expressed at weaker levels in migrating
674 rhombic lip-derived cells. NF1 was expressed in the hindbrain choroid plexus (cp)
675 across the developmental stages, from E12.5 to the adult stage. Mes, mesencephalon;
676 rl, rhombic lip; ml, molecular layer; gcl, granular cell layer; egl, external granular cell
677 layer; igl, internal granular cell layer. Scalebars: 200μm (E,F,G,H,I,J); 50μm (E'-F");
678 20μm (G'-H", I'-J'').
679
680 **Figure 5: NF1 is expressed in cerebellar neuronal lineages across development**
681 (A-D") NF1 was expressed in Purkinje cells across development, and arrowheads show
682 its colocalization with Calbindin (Calb). Insets show magnified views of one Calb$^+$
683 Purkinje cell across development and its colocalization with NF1. (E-H") Colabelling
684 NF1 with NeuN marking cerebellar granule cells showed no or low coexpression across
685 development. (I-L") NF1 expression was predominant in the mature neurons of deep
686 cerebellar nuclei (DCN) across development, colocalizing with NeuN (cream dashed
687 circles). NeuN$^+$ mature cells were not observed here at P0. (M,N) Schematics
688 demonstrate morphology and differential lamination of developing (<P21) and
689 developed (>P21) mouse cerebella. Mes, mesencephalon; rl, rhombic lip; ml, molecular

690 layer; gcl, granular cell layer; egl, external granular cell layer; igl, internal granular cell
691 layer; bv, blood vessels; cp, choroid plexus; bg, Bergmann glia. Scalebars: 25μm (A-B",
692 E-F"); 10μm (C-D", G-L").
693
694 **Figure 6: NF1 is expressed in the embryonic cerebellar ventricular progenitors**
695 (A,D) Schematics demarcate different germinal zones of cerebellar anlage at E14.5 and
696 E12.5. At E12.5, the cerebellar ventricular zone is subdivided into the zone producing
697 Purkinje cells (deep blue) and the interneuron-producing zone (light blue). (B-B", E-E")
698 NF1 is expressed perinuclearly in Sox2$^+$ progenitors in the cerebellar ventricular zone at
699 E12.5 and E14.5. However, NF1 was not expressed in Pax6$^+$ secondary progenitor cells
700 derived from the rhombic lip. Mes, mesencephalon; NTZ, nuclear transitory zone; 4V,
701 fourth ventricle; cvz, cerebellar ventricular zone. Scalebars: 20μm (B-F").
702
703 **Figure 7: NF1 is expressed in cerebellar glial lineages**
704 (A-H'') NF1 was expressed in a subset of Olig2$^+$ oligodendrocytes in both folium (A-D")
705 and deep cerebellar nuclei (E-H") at mature (P35) and developing (P12) mouse
706 cerebella (arrowheads). In magnified views (B-B",D-D",F-F",H-H"), cream dashed circles
707 mark NF1$^+$Olig2$^+$ double-positive oligodendrocytes, while red dotted circles mark Olig2$^+$
708 oligodendrocytes that did not express NF1. (I-N") NF1 was also expressed in the soma
709 and projection of the Bergmann glia across development. Colocalization with Blbp is
710 shown using arrowheads. ml, molecular layer; gcl, granular cell layer; egl, external
711 granular cell layer; igl, internal granular cell layer; pcl, Purkinje cell layer; wm, white
712 matter. Scalebars: 25μm (A-A", C-C", E-E", G-G", I-I", K-K", M-M"); 10μm (B-B", D-D", F-
713 F", H-H", J-J", L-L", N-N").
714
715 **Figure 8: Nf1 expression in murine optic cup and olfactory bulb**
716 (A,B) Schematics showing zones and cell layers of neurosensory organs, eye and
717 olfactory bulb. (C,F") NF1 is expressed in the developing mouse eye, predominantly in
718 the lens (L) and neuroretina (NR), which includes the photoreceptor layer (PRC), retinal
719 ganglionic cells and Müller glial cells in the broad retinal ganglionic cell layer (RGC) at
720 E17.5 and E14.5. Magnified insets (D-D", F-F") show colocalization of NF1 and Tbr2 in
721 the lens and a subset of intrinsically photosensitive RGCs. NF1 also showed wide
722 coexpression with Sox2 in PRC and retinal pigmented epithelium (RPE), but not with
723 the interneurons of neuroretina. NF1 colocalized with Tbr2 in the lens and a subset of
724 (G-J) NF1 was expressed strongly across the postnatal development of the olfactory
725 bulb. It showed strong expression in the mitral cell layer (MCL) of the main olfactory
726 bulb (MOB) and also in the accessory olfactory bulb (AOB). (K,L,O-P") Colabelling with
727 NeuN at P35 and P12 identified subsets of mitral cells that were double positive for NF1
728 and NeuN (arrowheads). (M,N, Q-R") Strong coexpression with Pax6 was seen in
729 posterior AOB (pAOB) at P0 and P3, but not in the other parts of MOB. IN, interneurons;

730 aAOB, anterior accessory olfactory bulb; EPL, external plexiform layer; GCL, granule
731 cell layer; GL, glomerular layer. Scalebars: 200μm (G,H,K,L); 100μm (C-C", E-E",
732 I,J,M,N); 50μm (O-O", P-P"); 25μm (Q-R"); 20μm (D-D", F-F").
733
734 **Figure 9: Reanalysis of single nuclei RNAseq data showing expression of *Nf1* in**
735 **adult mouse brain**
736 (A**,**F) UMAP plot for single nuclei RNAseq data from adult mouse cortex and
737 cerebellum, respectively. Transcriptionally distinct clusters were coloured based on cell
738 type. (B,G) UMAP plot illustrating the expression level of *Nf1* (red) across different
739 cortical and cerebellar clusters, respectively. (C-E) *Nf1* expression is higher in cortical
740 interneurons, differentiating OPCs, and excitatory neurons of adult murine cortex
741 compared to other neural populations. (H-J) In the adult murine cerebellum, *Nf1*
742 expression is enriched primarily in Purkinje cells, Golgi INs, Bergmann glia, and OPCs.
743 MGE_INs, medial ganglionic eminence interneurons; dMGE_INs, dorsal medial
744 ganglionic eminence interneurons; CGE_INs, caudal ganglionic eminence interneurons;
745 OPCs, oligodendrocyte precursor cells; MLI, molecular layer interneurons; PLI, Purkinje
746 layer interneurons; INs, interneurons; UBC, unipolar brush cells.
747

FIGURES

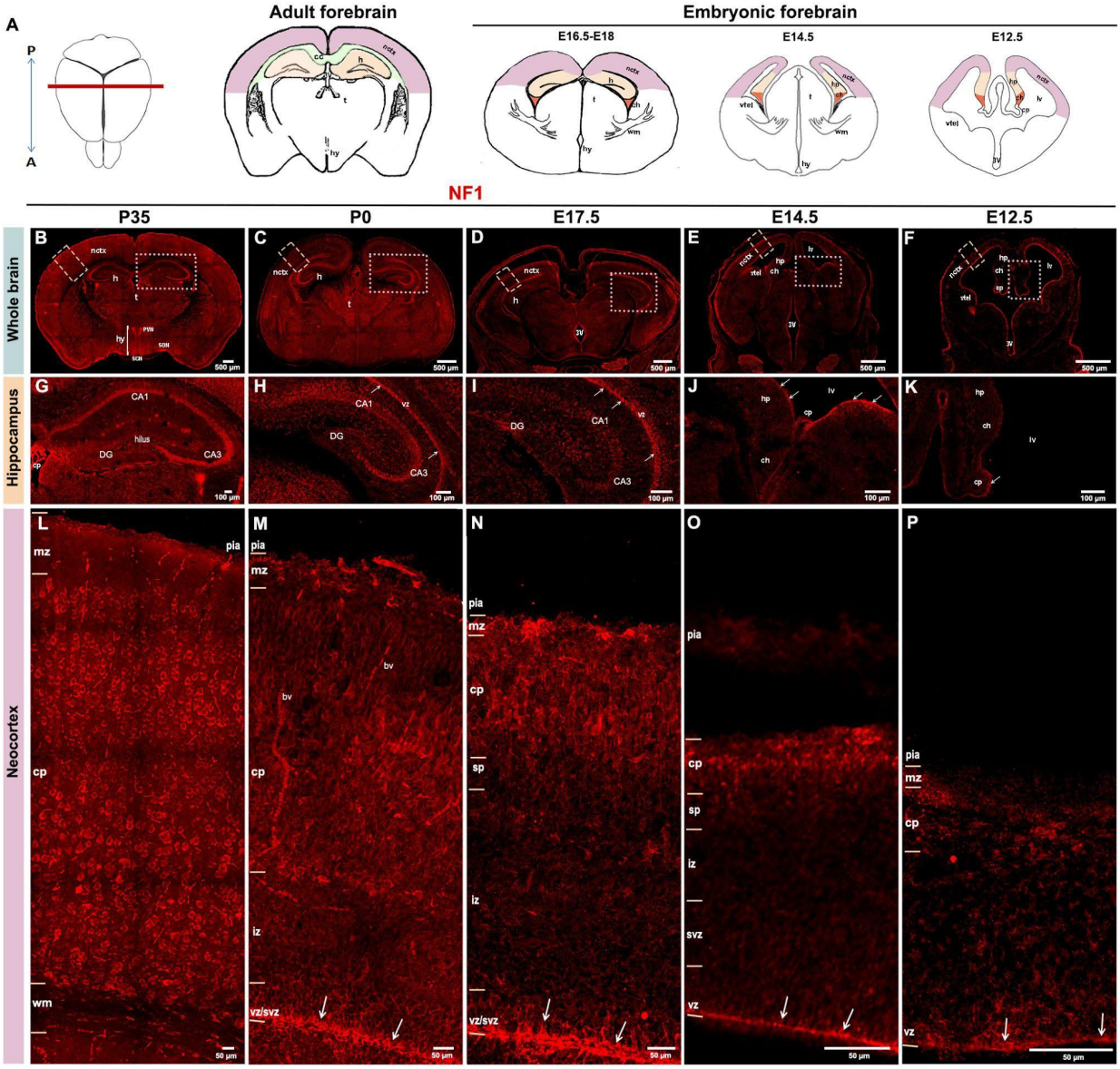

Figure 1

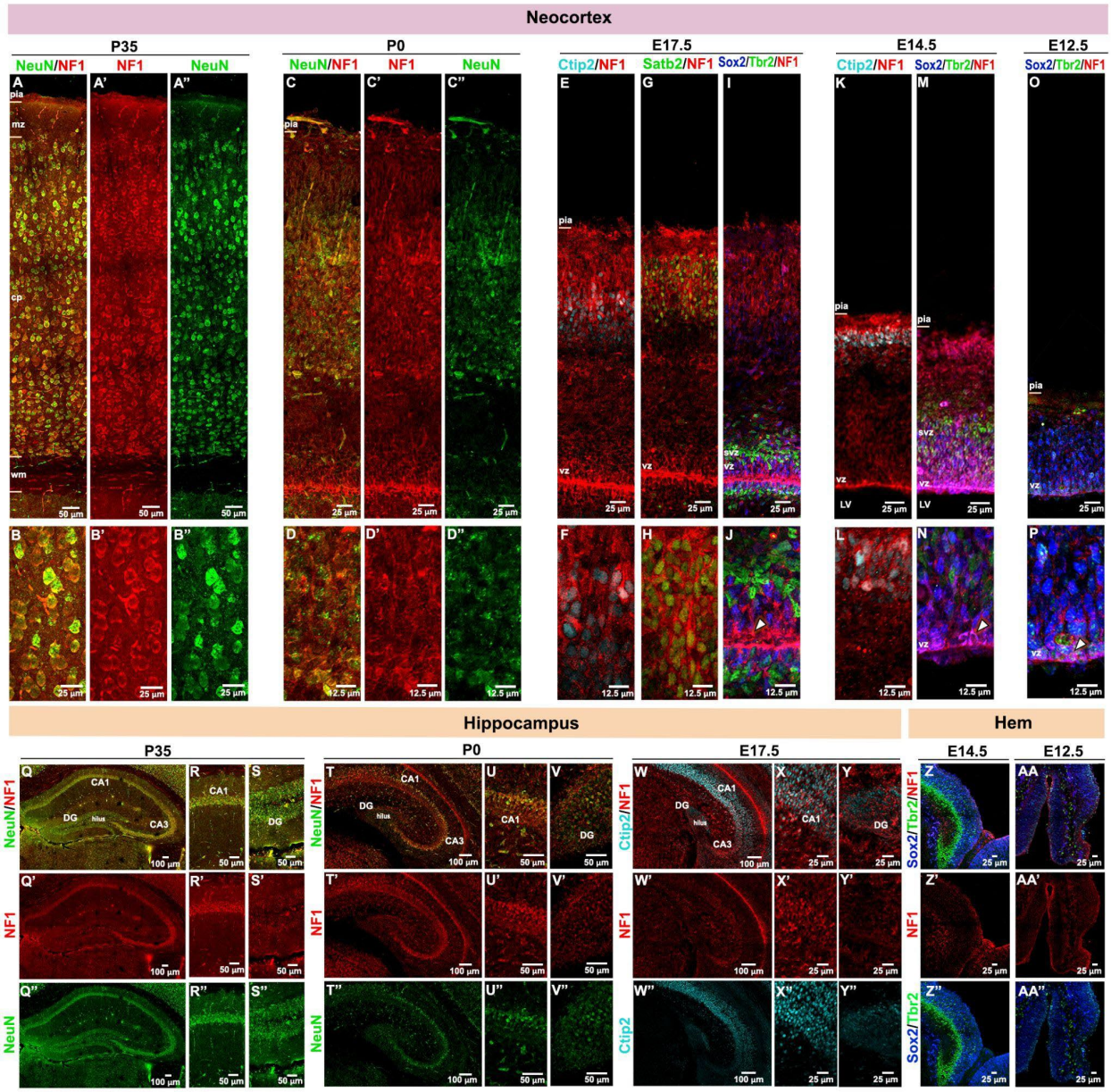
Neocortex
P35
NeuN/NF1
NF1
NeuN
P0
NeuN/NF1
NF1
NeuN
E17.5
Ctip2/NF1
Satb2/NF1
Sox2/Tbr2/NF1
E14.5
Ctip2/NF1
Sox2/Tbr2/NF1
E12.5
Sox2/Tbr2/NF1
pia
mz
cp
wm
vz
svz
LV
Hippocampus
Hem
CA1
CA3
DG
hilus
NeuN/NF1
NF1
NeuN
Ctip2/NF1
Ctip2
Sox2/Tbr2/NF1
Sox2/Tbr2

Figure 2

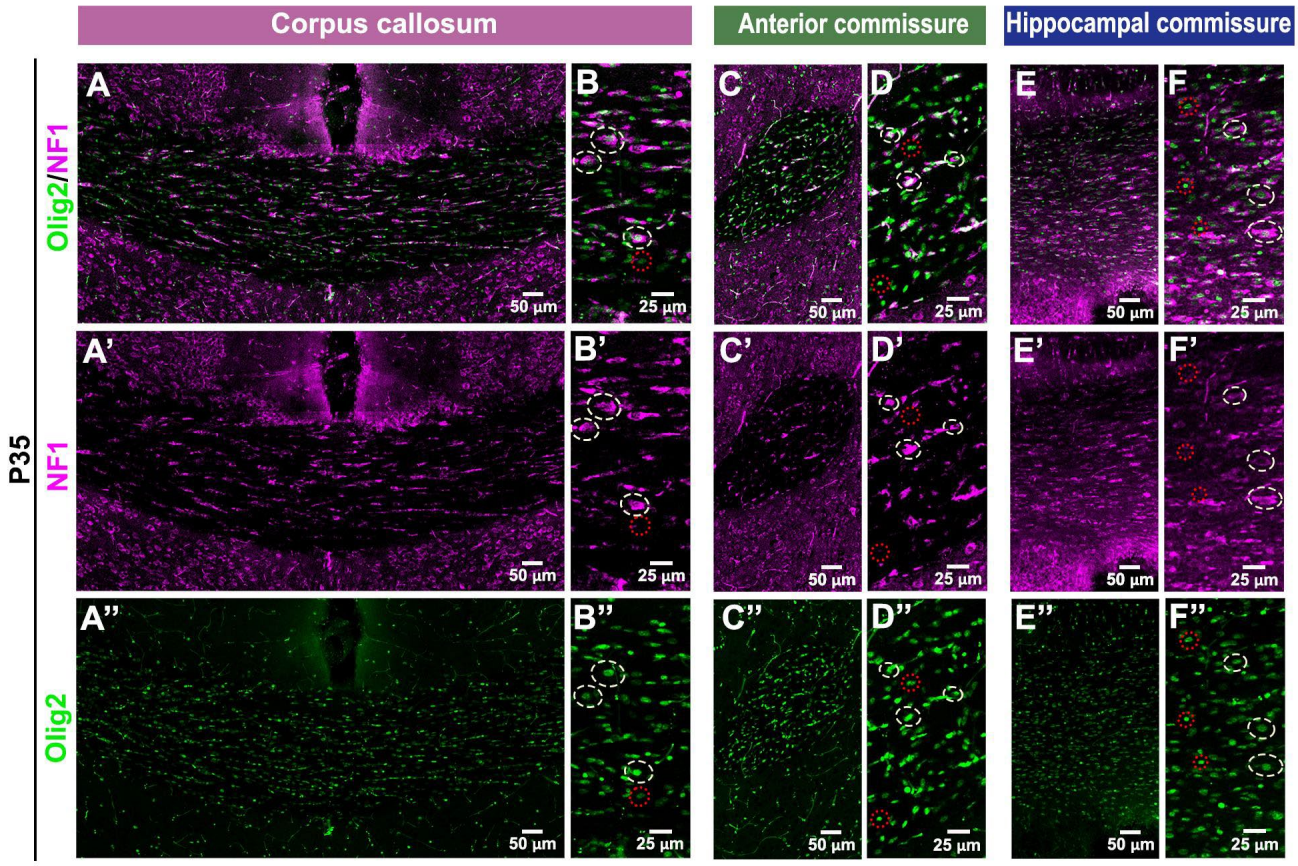
Corpus callosum
Anterior commissure
Hippocampal commissure
P35
Olig2/NF1
NF1
Olig2
A
B
C
D
E
F
A'
B'
C'
D'
E'
F'
A''
B''
C''
D''
E''
F''
50 µm
25 µm

Figure 3

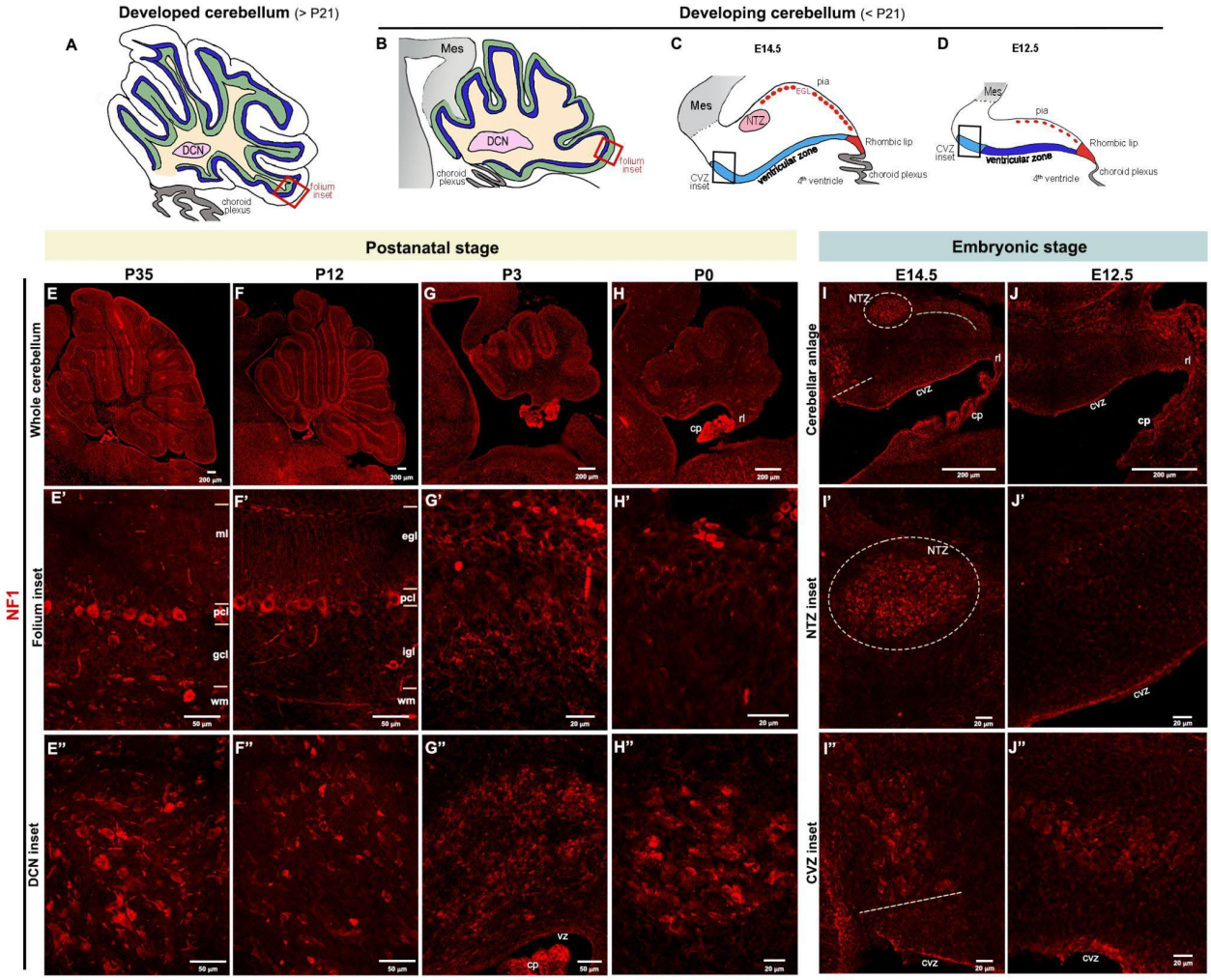
Developed cerebellum (> P21)
Developing cerebellum (< P21)
A
B
C
D
E14.5
E12.5
Mes
DCN
NTZ
pia
egl
Rhombic lip
ventricular zone
CVZ inset
4th ventricle
choroid plexus
folium inset
Postanatal stage
Embryonic stage
P35
P12
P3
P0
E14.5
E12.5
Whole cerebellum
Folium inset
DCN inset
Cerebellar anlage
NTZ inset
CVZ inset
NF1
ml
pcl
gcl
wm
egl
igl
rl
cp
cvz
vz

Figure 4

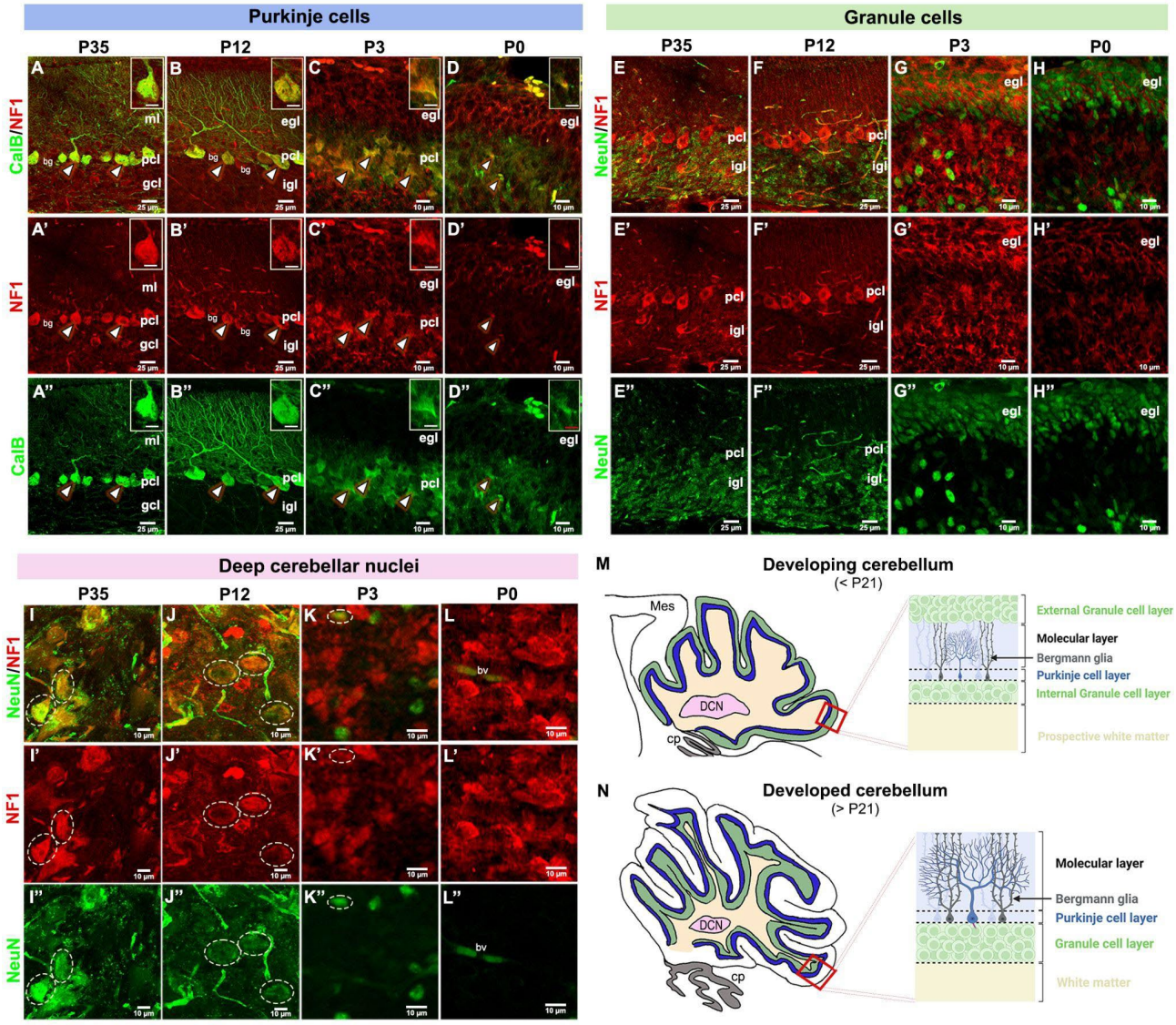
Purkinje cells
Granule cells
P35
P12
P3
P0
CalB/NF1
NF1
CalB
NeuN/NF1
NeuN
ml
pcl
gcl
igl
egl
bg
Deep cerebellar nuclei
bv
M
Developing cerebellum
(< P21)
Mes
DCN
cp
External Granule cell layer
Molecular layer
Bergmann glia
Purkinje cell layer
Internal Granule cell layer
Prospective white matter
N
Developed cerebellum
(> P21)
Molecular layer
Bergmann glia
Purkinje cell layer
Granule cell layer
White matter

Figure 5

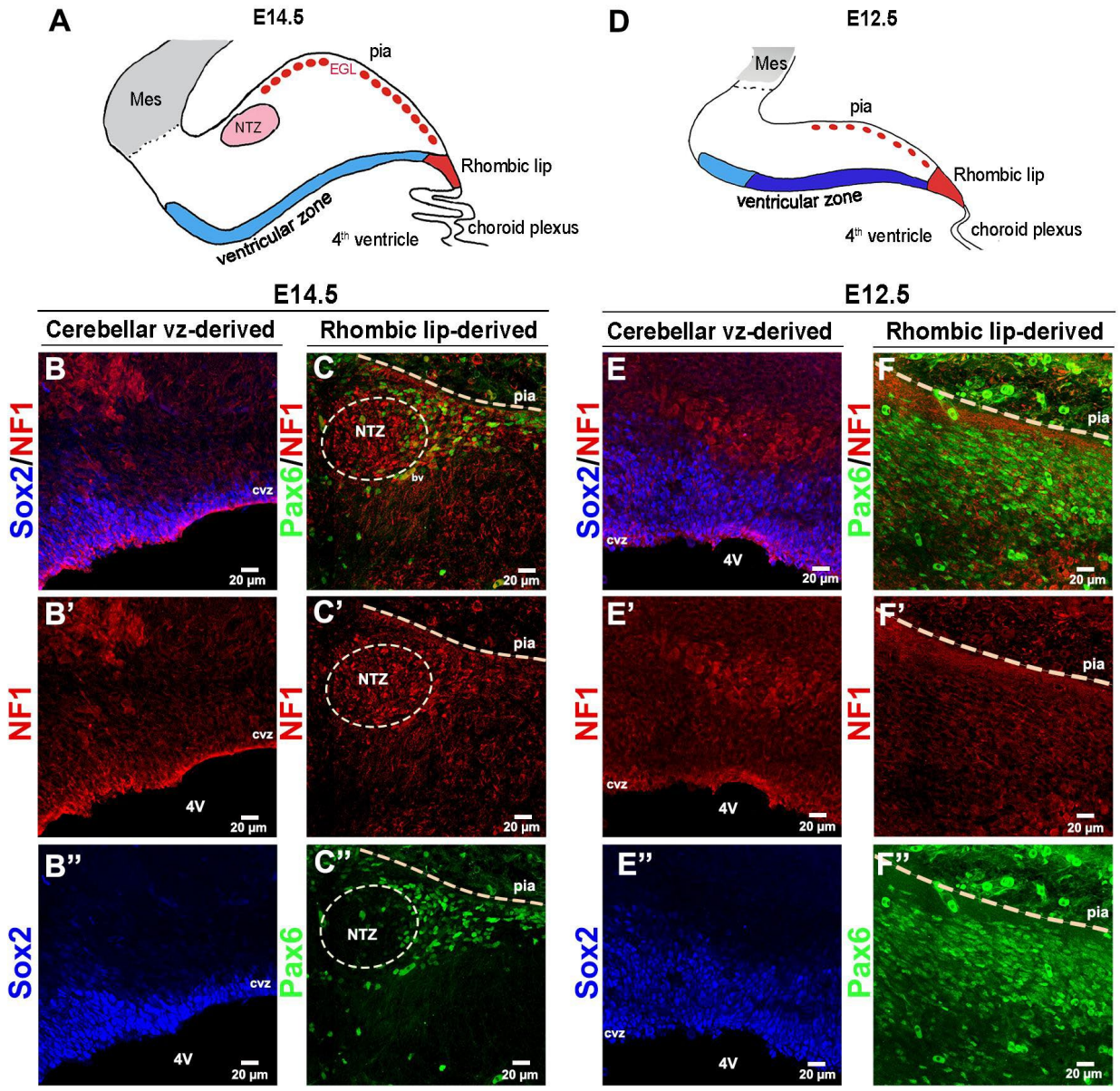
A
E14.5
Mes
NTZ
EGL
pia
Rhombic lip
ventricular zone
4th ventricle
choroid plexus
D
E12.5
Mes
pia
Rhombic lip
ventricular zone
4th ventricle
choroid plexus
E14.5
Cerebellar vz-derived
Rhombic lip-derived
E12.5
Cerebellar vz-derived
Rhombic lip-derived
Sox2/NF1
Pax6/NF1
NF1
Sox2
Pax6
B
B'
B''
C
C'
C''
E
E'
E''
F
F'
F''
cvz
4V
NTZ
bv
pia
20 µm

Figure 6

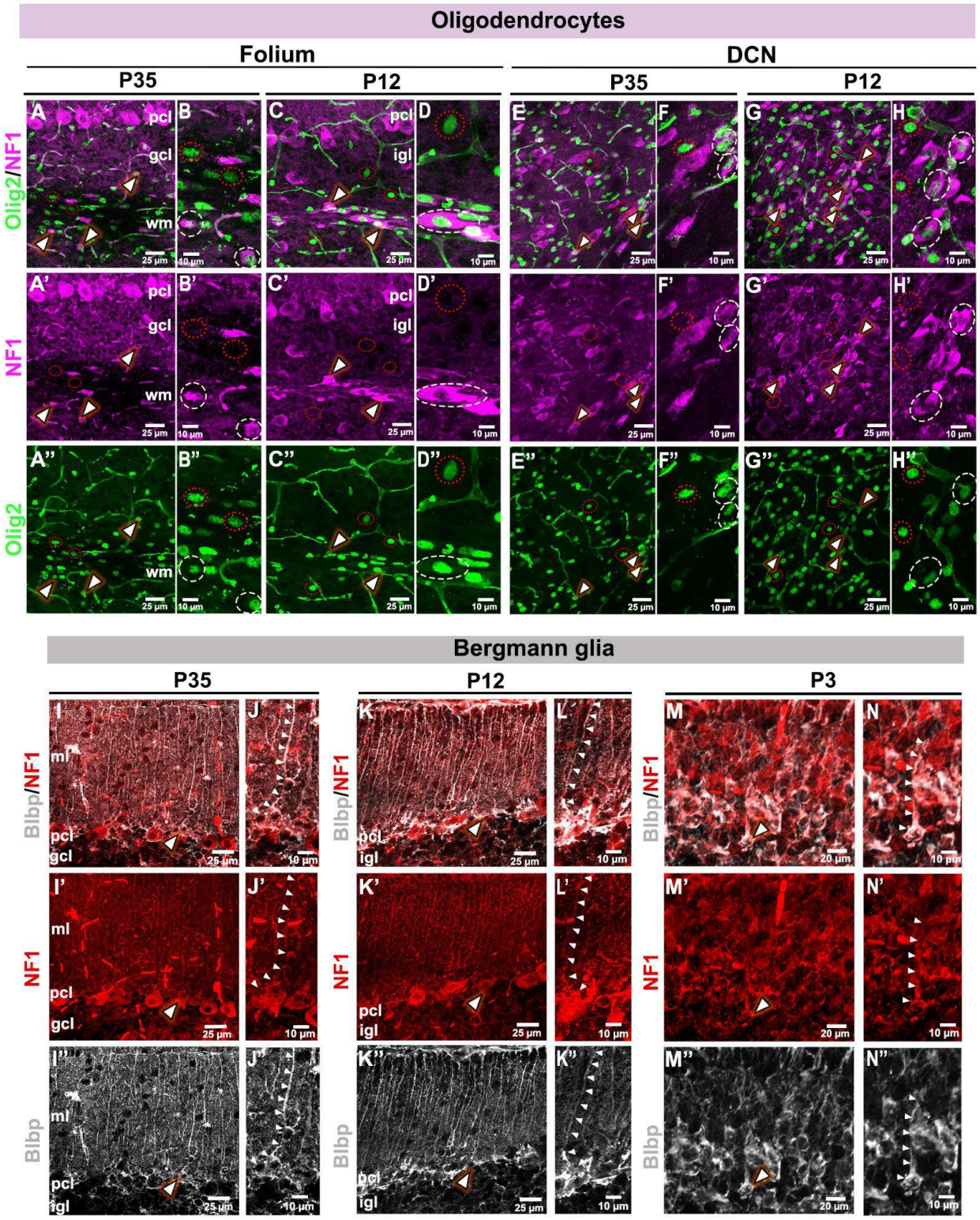
Oligodendrocytes
Folium
DCN
P35
P12
P35
P12
Olig2/NF1
NF1
Olig2
pcl
gcl
wm
igl
25 µm
10 µm
Bergmann glia
P35
P12
P3
Blbp/NF1
NF1
Blbp
ml
pcl
gcl
igl
25 µm
10 µm
20 µm

Figure 7

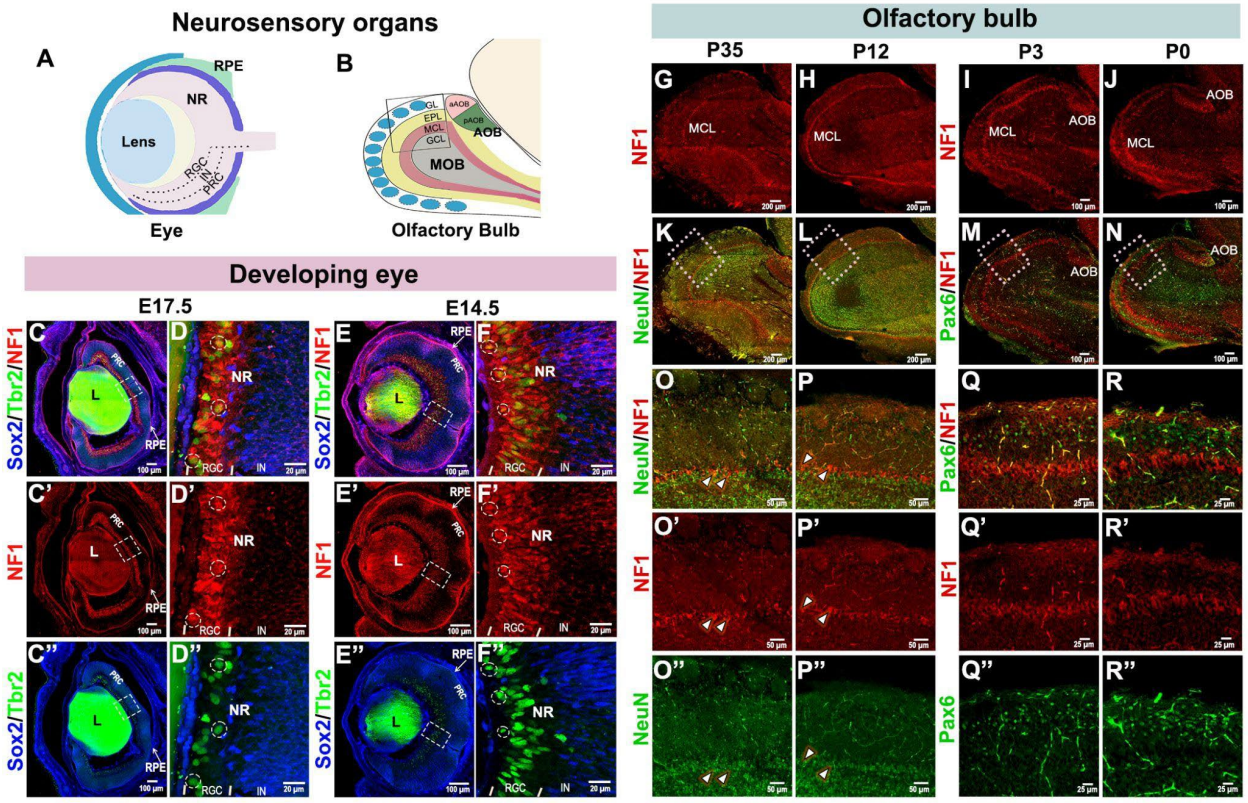
Neurosensory organs
A
RPE
NR
Lens
RGC
IN
PRC
Eye
B
GL
aAOB
EPL
pAOB
MCL
GCL
AOB
MOB
Olfactory Bulb
Developing eye
E17.5
E14.5
Sox2/Tbr2/NF1
NF1
Sox2/Tbr2
C
C'
C''
D
D'
D''
E
E'
E''
F
F'
F''
L
RPE
PRC
NR
RGC
IN
Olfactory bulb
P35
P12
P3
P0
NeuN/NF1
Pax6/NF1
NeuN
Pax6
G
H
I
J
K
L
M
N
O
P
Q
R
O'
P'
Q'
R'
O''
P''
Q''
R''
MCL
AOB

Figure 8

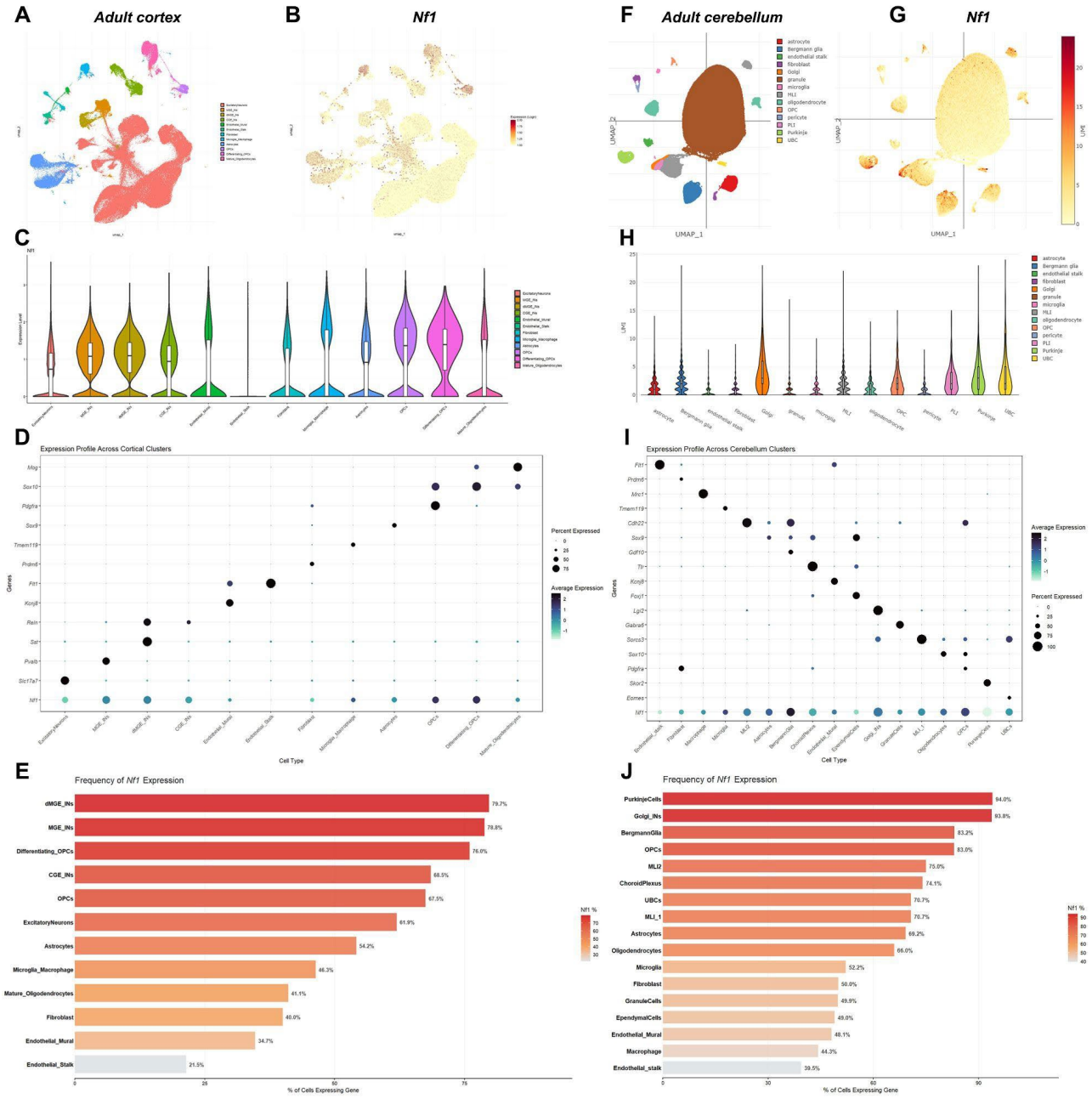
A
Adult cortex
B
Nf1
F
Adult cerebellum
G
Nf1
C
D
Expression Profile Across Cortical Clusters
Percent Expressed
Average Expression
Genes
Cell Type
E
Frequency of Nf1 Expression
dMGE_INs 79.7%
MGE_INs 78.8%
Differentiating_OPCs 76.0%
CGE_INs 68.5%
OPCs 67.5%
ExcitatoryNeurons 61.9%
Astrocytes 54.2%
Microglia_Macrophage 46.3%
Mature_Oligodendrocytes 41.1%
Fibroblast 40.0%
Endothelial_Mural 34.7%
Endothelial_Stalk 21.5%
Nf1 %
% of Cells Expressing Gene
H
I
Expression Profile Across Cerebellum Clusters
Average Expression
Percent Expressed
Genes
Cell Type
J
Frequency of Nf1 Expression
PurkinjeCells 94.0%
Golgi_INs 93.8%
BergmannGlia 83.3%
OPCs 83.0%
MLI2 75.0%
ChoroidPlexus 74.1%
UBCs 70.7%
MLI_1 70.7%
Astrocytes 69.2%
Oligodendrocytes 66.0%
Microglia 52.2%
Fibroblast 50.0%
GranuleCells 49.9%
EpendymalCells 49.0%
Endothelial_Mural 48.1%
Macrophage 44.3%
Endothelial_stalk 39.5%
Nf1 %
% of Cells Expressing Gene

Figure 9